Effect of carbonation curing regime on electric heating performance of CNT/cement composites

Daeik Jang [a], H.N. Yoon [a], Joonho Seo [a], Beomjoo Yang [b], Jeong Gook Jang [c],[**], Solmoi Park [d],[*]

[a] *Department of Civil and Environmental Engineering, Korea Advanced Institute of Science and Technology (KAIST), 291 Daehak-ro, Yuseong-gu, Daejeon, 34141, Republic of Korea*
[b] *School of Civil Engineering, Chungbuk National University, 1 Chungdae-ro, Seowon-gu, Cheongju, Chungbuk, 28644, Republic of Korea*
[c] *Division of Architecture and Urban Design, Urban Science Institute, Incheon National University, 119 Academy-ro, Yeonsu-gu, Incheon, 22012, Republic of Korea*
[d] *Department of Civil Engineering, Pukyong National University, 45 Yongso-ro, Nam-gu, Busan, 48513, Republic of Korea*

ARTICLE INFO

ABSTRACT

Carbonation curing is a widely used technique in the construction industry due to its effect in trapping CO_2 in cement matrixes and reducing carbon emissions. However, the use of carbonation curing in the production of functional cementitious composites has rarely been reported. Herein, the effects of carbonation curing regime on the electric heating performances of carbon nanotube (CNT)/cement composites are investigated. Four different CNT contents are used to fabricate the samples, and the samples are cured under three different curing conditions. The electrical and thermal conductivities as well as compressive strengths of the samples are examined. Their physicochemical properties are investigated via X-ray diffraction and thermogravimetric analyses, and their CO_2 uptake levels are calculated. The electric heating performance is evaluated in terms of maximum heating temperature and heat-induced electrical resistivity under cyclic heating condition. Results show that the CO_2 uptake levels increase with the amount of CNT since the CNT can develop the porous structures, and it can increase the environmental impact reduction level. Meanwhile, an excessive CO_2 curing can decrease the electrical conductivity and lower the electrical heating performance of the samples. In addition, the CO_2 uptake level is significantly affected by the percolation threshold of the CNT. In this context, the CO_2 curing regime is required to set based on the intended functionality of the CNT/cement composites.

1. Introduction

Conductive cementitious composites have garnered increasing attention owing to their potential for a wide range of applications, such as cement-based sensors for monitoring structural health [1,2], electrical heating systems for road and/or pavement de-icing systems in cold regions [3,4], and electromagnetic wave interference shielding composites [5,6]. Various conductive fillers (e.g., carbon black, graphite, steel fiber, and carbon fiber) have been used to fabricate conductive cement composites to form conductive networks and secure conductive properties [7,8]. However, large amounts of conventional fillers are required to ensure favorable electrical conductivity in the cement composites for functional purposes [7,8]. Hence, many studies have focused on using carbon nanotube

---

(CNT), which exhibit excellent electrical and thermal properties [9], due to their high aspect ratios [10,11]. Owing to the advantages of CNT, they have been considered as an alternative conductive filler that can mitigate the problems of conventional fillers [12,13].

Recently, carbonation curing has been used extensively in the construction field as it can effectively trap CO_2 in a cement matrix and can reduce carbon emissions [14]. In addition, carbonation curing can accelerate the hydration of cement clinkers (e.g., dicalcium silicate (C_2S) and tricalcium silicate (C_3S)), which improves the mechanical strength and durability of cement-based structures [14–16]. Chen et al. reported that the appropriate carbonation curing increased compressive strength of cement paste at early ages; however, the excessive carbonation curing led to the decalcification and/or decomposition of C–S–H, decreasing the compressive strengths [15]. In addition, Chen and Gao investigated the effect of carbonation curing extent on changes of microstructure of cement paste, reporting that the suitable carbonation duration is required to improve the compressive strengths of cement paste [16].

Meanwhile, some researchers have investigated that the effect of weathering carbonation on the changes of electrical conductivity of CNT/cement composites. Lee et al. [17] observed that the electrical resistivity increased as CNT/cement composites were exposed to weathering carbonation over 120 days, indicating the carbonation effect is significant on the changes of electrical conductivity. In addition, Gawel et al. [18] reported that the carbonation products (i.e., calcium carbonate) can strongly affect the formation of conductive networks in the composites, disturbing the flow of electrical current. Thus, it can be inferred from the previous studies that the carbonation can hinder the connection of the adjacent CNT particles, decreasing the electrical conductivity. Although some efforts have demonstrated the changes in the electrical conductivity of CNT/cement composites that have experienced weathering carbonation, few studies have investigated the effects of carbonation curing regime on the changes of electrical conductivity of CNT/cement composites. It is deduced from the relevant studies conducted recently that the carbonation-cured CNT/cement composites are expected to be used in various functional purposes with both effectively trapping CO_2 and reducing carbon emissions, given that the composites can achieve their original electrical and thermal conductivities. In addition, to the best of our knowledge, the use of carbonation curing in the production of functional cementitious composites has rarely been reported.

In this regard, this study is performed to investigate the effects of carbonation curing regime on electrical heating performance of CNT/cement composites. Four different CNT amount (0.1, 0.3, 0.6, or 1.0%) and three different carbonation curing regime based on the number of carbonation curing days are used to fabricate the samples. Subsequently, the effects of carbonation curing regime on the characterization and physicochemical properties of the composites are investigated. X-ray diffraction (XRD) and thermogravimetric (TG) analyses are conducted to facilitate comprehensive discussions regarding the effects of carbonation curing regime on the characterization as well as physicochemical and electrical heating performance of CNT/cement composites. In addition, field emission-scanning electron microscopy (FE-SEM) is performed to capture the microstructural images of the functional CNT/cement composites in such that carbonation-induced hydrates and the formation of conductive networks can be investigated systematically.

2. Experimental program

2.1. Sample preparation

Ordinary Portland cement (PC) was used as the binder material in accordance with ASTM C150. CNT (Jeio Co. Ltd.) with diameters of approximately 10 nm and lengths of 100–200 μm were selected as conductive fillers, and their specifications are listed in previous publications [19,20]. Silica fume was added to improve the mechanical properties of the composites and enhance the dispersion of CNT [21]. A polycarboxylate-type superplasticizer (SP; Dongnam Co. Ltd.) was used to reduce the amount of water required and improve the dispersion of CNT [22]. The mix proportions used to fabricate the samples are summarized in Table 1, where the number indicates the amount of CNT in the sample. The water-to-cement ratio was varied from 0.22 to 0.40 based on the amount of CNT to regulate the target flow of the mixtures (i.e., 110 ± 5 mm) and maximize the shear forces between the mixtures and the CNT-agglomerates, thereby improving the dispersion of CNT agglomerates in the composites [12]. Thereafter, direct mechanical mixing was performed to improve the dispersion of the CNT particles while considering the limitations of ultrasonication [17,23,24].

The samples were fabricated as follows: raw materials including cement, silica fume, and CNTs were added to a standard Hobart mixer and mixed for 5 min at a low speed. Subsequently, a solution comprising water and a SP was prepared and poured into the mixture. The mixture was mixed for 5 min at a low speed and then for 5 min at a high speed. Next, the mixture was poured into a 50 mm cubical mold. Copper-type electrodes measuring 70 mm long and 20 mm wide were prepared by coating them with silver paste to minimize contact resistance between the electrodes and the composite. The electrodes were embedded into the composite to depths of 50 and 20 mm between the two electrodes. The samples were encapsulated to prevent water evaporation and then cured in an oven at 25 °C for 1 d. After curing, they were demolded and categorized into three groups according to the carbonation curing condition and thus the extent of carbonation (non-carbonated, partially-carbonated, and fully-carbonated). The samples in the non-carbonated group were cured in the same oven as described above. The fully and partially-carbonated samples were cured in a carbonation cham-

Table 1
Mix proportions of the samples (wt%).

Sample Code	Cement	Silica fume	CNT	Water	SP	Target flow (mm)
C0.1	100	10	0.1	22	2	110 ± 5
C0.3	100	10	0.3	25	2	
C0.6	100	10	0.6	28	2	
C1.0	100	10	1.0	40	2	

ber with an atmospheric CO_2 concentration of 10%, temperature of 25 °C, and relative humidity of 60% from days 1st and 7th day after demolding to 28th day, respectively, to vary the extent of carbonation [25,26].

2.2. Test methods

The electrical resistances were measured using a portable multimeter (Keysight U1282A) and converted to electrical resistivity using a previously reported formula to account for the dimensions of the electrodes [27–29]. A TPS 2500 S device (Gothenburg) was used to measure the thermal conductivity based on the ISO standard 22007-2 [30]. The compressive strengths were measured using a universal testing machine (INSTRON) at a constant loading rate of 0.01 mm/s. The electrical resistance, thermal conductivity, and compressive strength measurements were repeated for three specimens, and the averages were calculated as representative values.

The physicochemical properties of the composites were investigated via XRD and TG/DTG. XRD patterns were obtained using an EMPYREAN device (Malvern Panalytical) with CuKα radiation. A generator voltage of 40 kV and a tube current of 30 mA were applied, and the device was rotated from 5° to 65° (2θ angle) at an interval of 0.026° and 1.56 per step. TG analysis was performed using a Labsys Evo TG-DTA device (SETARAM), and the relative weight change of the samples was measured in the temperature range of 25 °C–800 °C. For the XRD and TG/DTG analysis, the powder samples smaller than 63 μm in size were prepared by grinding manually. The prepared powder samples were then placed in a carbonation chamber to ensure a uniform degree of carbonation. Microstructural images of the fractured samples were obtained using FE-SEM (Hitachi S4800). For the FE-SEM observations, fractured samples were prepared based on recommendations from RILEM [31].

In the electrical heating test, an input voltage of 8 V was applied for 1 h using a DC power supply (PL-3005S). The surface temperature measured using the K-type thermocouple was recorded every 5 s using a data logger (Agilent Tech, 34972A). The heating process was repeated for 10 cycles to examine the cyclic heating stability. During the heating test, the electrical resistances of the composites before heating and after 1 h of heating were measured, which correspond to the "initial" and "terminal" electrical resistances, respectively. Furthermore, their electrical stability during long-term heating was tested over 20 h.

3. Results and discussions

3.1. Characterization of the samples

Samples with different CNT contents were fabricated to determine the percolation thresholds. The electrical resistivities of the samples during 28 d of curing and on the 28th day, are shown in Fig. 1. The electrical resistivity increases with the curing time because the hydrates in the samples disconnected the CNTs [19]. As shown in Fig. 1 (b), the electrical resistivity reduces significantly when the CNT amount is 0.1–0.3 wt%, which indicates the percolation threshold range. The amount of CNT for this percolation threshold is equal to or less than the results reported previously, indicating that the CNT particles dispersed uniformly in the samples [32–34]. The effects of carbonation extent on the electrical resistivity, are shown in Fig. 2. Regardless of the amount of CNT, the period of carbonation curing significantly affected the electrical resistivity. However, the effects were more conspicuous in the samples with lower CNT amounts (i.e., 0.1 wt% and 0.3 wt%) as compared with those with higher CNT contents (i.e., 0.6 wt% and 1.0 wt%). The electrical resistivities of the C0.1 and C0.3 samples cured under non-carbonated, partially-carbonated, and fully-carbonated conditions were 2120, 3028, and 3101 Ω cm, and 192, 218, and 264 Ω cm, respectively. By contrast, the electrical resistivities of the corresponding C0.6 and 1.0 samples were 51, 57, and 53 Ω cm, and 23, 25, and 30 Ω cm, respectively. This effect can be explained by the percolation threshold shown in Fig. 1 (b). Denser conductive CNT networks formed in the samples with CNT amounts exceeding the percolation threshold (i.e., 0.6 wt% and 1.0 wt%) owing to the excessive amount of available CNTs. Thus, the CNTs were in much closer proximity to each other as compared with those in the samples with lower CNT amounts (i.e., 0.1 wt% and 0.3 wt%). Accordingly, as dense conductive networks developed, the effects of precipitation of carbonation products on the electrical resistivity deteriorated, which is attributable to the tunneling effect [35]. In this regard, even if carbonation products are formed in the samples with higher CNT amounts and hindered the movement of electrons, the electrons can skip over them owing to the tunneling effect, which will become more prominent as the CNT amount increases [35]. Therefore, the extent of carbonation exerts a less significant effect on the electrical resistivity as the CNT content increases.

The thermal conductivities of the samples with varying extents of carbonation samples based on different numbers of carbonation curing days are shown in Fig. 3. As shown, the thermal conductivity increases as the CNT content increases from 0.1 wt% to 0.6 wt%; however, it decreases when an excessive amount of CNT is added (i.e., 1.0 wt%). As shown in Table 1, the water-to-cement ratio increases from 0.22 to 0.40 to maintain the target flow. A similar water-to-cement ratio was used for the C0.1, C0.3, and C0.6 samples, but the ratio used in the C1.0 sample was much higher. Thus, the effect of the water-to-cement ratio is negligible when comparing the thermal conductivities of C0.1, C0.3, and C0.6 samples. For these samples, the thermal conductivity increased with the CNT amount, since CNT possesses better thermal conductivity compared with other materials, such as cement and silica fume. Although C1.0 sample contained 1.0 wt% CNTs, its high water-to-cement ratio rendered it highly porous. The samples used for the thermal conductivity measurements were dried in an oven at 60 °C for 3 d to evaporate any residual water and mitigate its effect on the results. The high porosity of C1.0 might have contributed to its lower thermal conductivity. Meanwhile, the partially- and fully-carbonated samples exhibited lower thermal conductivities than the non-carbonated samples. This is because carbonation-induced hydrates had developed in the partially and fully carbonated samples. The hydrates possess a much lower thermal conductivity than the CNT, and they can hinder the formation of CNT-based thermal networks, thereby increasing the thermal resistance and decreasing the effective thermal conductivity.

The compressive strengths of the samples fabricated based on different numbers of carbonation curing days are shown in Fig. 4. As shown, the compressive strength decreases as the CNT amount increases. In particular, the compressive strengths of C0.6 and C1.0
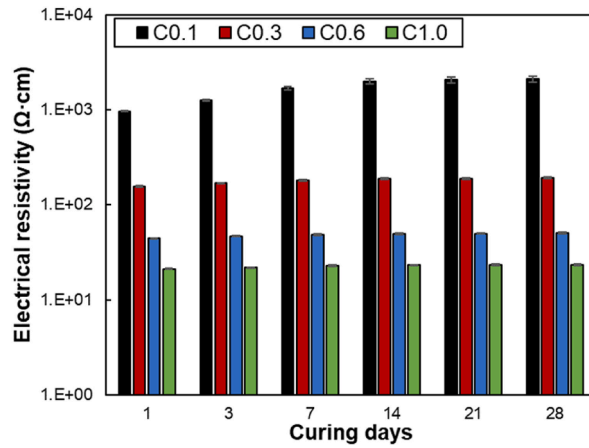
(a)
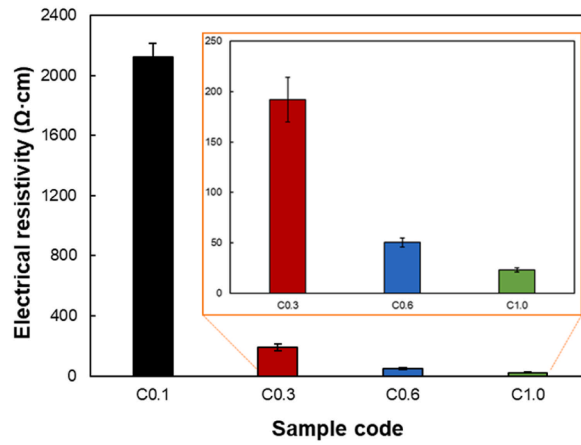
(b)

Fig. 1. Electrical resistivity of the samples: (a) cured over 28 d and (b) at 28 d of curing.
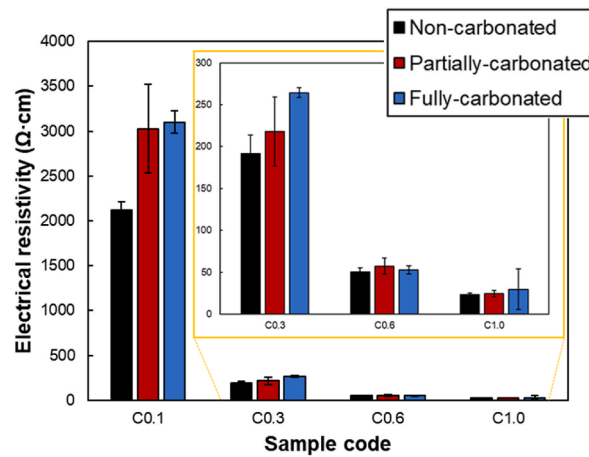

Fig. 2. Electrical resistivity of samples fabricated via carbonation curing extent.
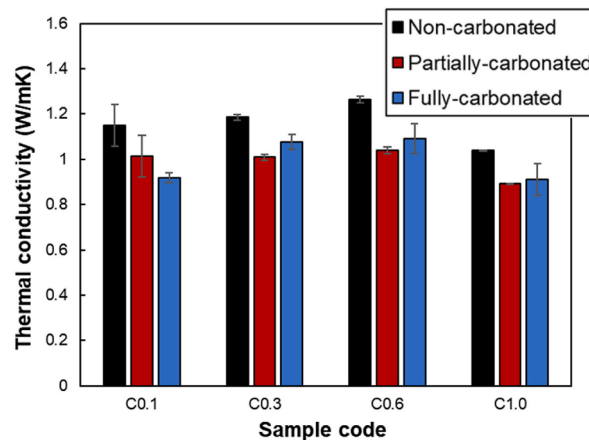
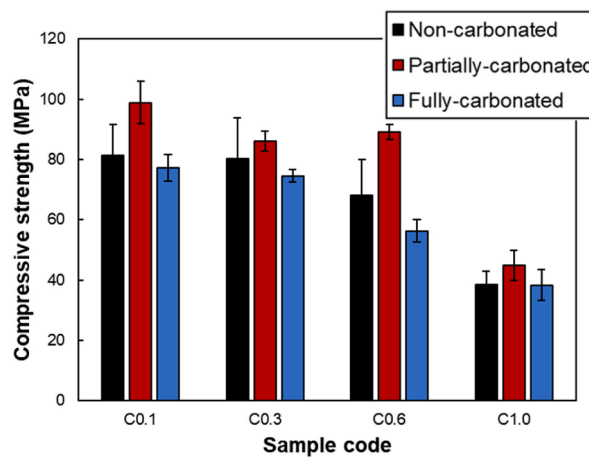Fig. 3. Thermal conductivity of samples fabricated via carbonation curing extent.

Fig. 4. Compressive strength of samples fabricated via carbonation curing extent.

samples are much lower than those of C0.1 and C0.3 samples. According to previous studies, a low amount of CNT can fill the pores as well as bridge the hydrates and microcracks in cementitious composites, which results in the formation of stiffer C–S–H in the composites, thereby improving their mechanical properties [36]. However, an excessive amount of CNTs leads to development of a porous structure, which may degrade their mechanical properties [37]. When the CNT amount exceeded 0.3 wt%, the porosity increased because the CNT content was above the percolation threshold (0.3 wt%–0.5 wt%), which resulted in the formation of CNT agglomerates. Hence, the compressive strengths of C0.6 and C1.0 decreased significantly by 16.3% and 52.48%, respectively. In addition, the effects of the carbonation curing extent on the changes in the compressive strength are shown in Fig. 4. The compressive strengths of the partially carbonated samples increased compared with those of the non-carbonated samples, i.e., increase percentages of 21.6%, 7.3%, 30.9%, and 16.3% were observed in C0.1, C0.3, C0.6, and C1.0 samples, respectively. Based on previous findings, the compressive strength of cementitious composites can be improved via carbonation curing as the latter may promote the hydration kinetics, and the results obtained in this study are similar to those obtained in previous studies [25,38]. By contrast, the compressive strengths of the fully-carbonated samples were lower than those of the non-carbonated samples by 4.96%, 6.93%, 17.21%, and 0.75% when CNT contents were 0.1, 0.3, 0.6, and 1.0 wt%, respectively (Fig. 4). Similar results were reported previously, i.e., excessive carbonation curing decreased the compressive strength of cementitious composites [15,16]. Excessive carbonation curing can cause the decalcification and/or decomposition of C–S–H in cementitious composites, which may consequently reduce their compressive strength [15,16]. The compressive strengths of the fully-carbonated C1.0 samples are similar to those of the non-carbonated samples (Fig. 4), indicating that the effect of carbonation curing is negligible. This is attributed to the relatively low compressive strengths of the non-carbonated C1.0 samples (38.64 MPa) arising from the excessive CNT amount, which increases the porosity and imposes a more significant effect than the decalcification and/or decomposition of C–S–H caused by carbonation curing.

The conductive networks in the CNT/cement composites were significantly affected by carbonation-induced hydrates. Thus, their microstructural images were captured using scanning electron microscopy (SEM), as shown in Fig. 5. The SEM images show that the well-dispersed CNT formed conductive networks in the samples, regardless of the number of carbonation curing days. Based on the electrical resistivity results shown in Fig. 2, an CNT content of 0.6 wt% exceeds the percolation threshold (i.e., 0.3 wt%–0.5 wt%); therefore, relatively dense and well-dispersed conductive networks were formed. In terms of hydrates, a high volume of C–S–H was
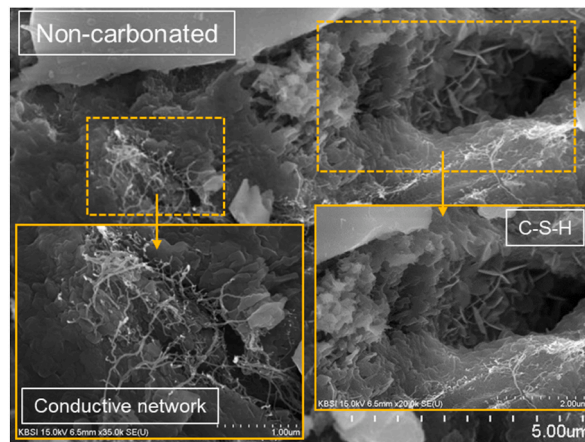
(a)
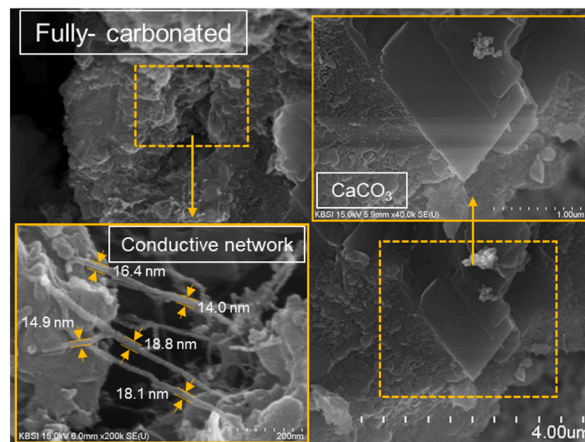
(b)

Fig. 5. SEM images of conductive networks and hydrates in (a) non and (b) fully carbonated C0.6 samples.

observed in the non-carbonated samples, while $CaCO_3$, as formed by carbonation curing, was abundantly observed in the fully carbonated samples. Although hydrates can affect the formation of conductive CNT networks, their effect is mitigated when the CNT content exceeds the percolation threshold. Thus, based on the test results observed in the present study, CNT amounts above the percolation threshold (>0.5 wt%) are recommended for the fabrication of conductive cementitious composites cured in a CO_2-rich environment, which requires a high and stable electrical conductivity for functional purposes.

3.2. Physicochemical properties of the samples

The XRD patterns of the samples exposed to different carbonation-curing conditions are shown in Fig. 6. The peaks can be classified into two main components: unreacted cement clinkers (e.g., alite (Ca_3SiO_5, PDF# 00-042-0551) and belite (Ca_2SiO_4, PDF# 00-029-0369)) and hydration products, such as ettringite ($Ca_6Al_2(SO_4)_3(OH)_{12}\cdot26H_2O$, PDF# 00-013-0350), portlandite ($Ca(OH)_2$, PDF# 00-044-1481), and calcite ($CaCO_3$, PDF# 01-081-2027). The main peaks corresponding to the presence of ettringite ($Ca_6Al_2(SO_4)_3(OH)_{12}\cdot26H_2O$, PDF# 00-013-0350) and portlandite ($Ca(OH)_2$, PDF# 00-044-1481) were observed in the non-carbonated samples, regardless of the embedded CNT amount. An increase in calcite was observed in the partially and fully-carbonated samples owing to the carbonation of portlandite [26]. In addition, the level of increase in calcite due to the carbonation reaction differs by the embedded CNT amount, indicating that a higher amount of calcite is formed when the CNT amount increases. This phenomenon can be deduced from the CNT-induced porosities in the composites. Undispersed CNT bundles in the composite can form CNT agglomerates, which may increase the porosity volume. Moreover, the addition of CNTs to hollow tubes can significantly increase the number of pores in the composites [20]. Thus, the high porosity formed in the composites with higher CNT amounts can accelerate CO_2 diffusion and carbonation kinetics.

The TG/DTG test results are shown in Fig. 7. Similar to previous studies, the results can be classified into three temperature regions: 100 °C-120 °C, 400 °C-450 °C, and 650 °C-750 °C [14]. The first temperature range is associated with the evaporation of mois-
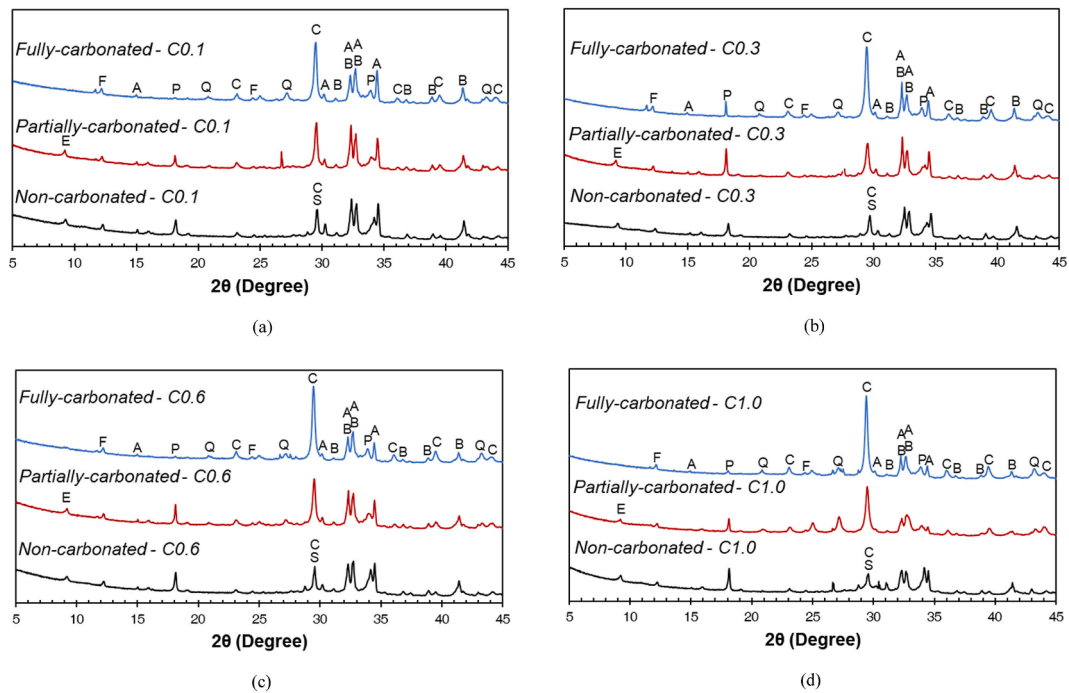
(a)

(b)

(c)

(d)

Fig. 6. XRD patterns of (a) C0.1, (b) C0.3, (c) C0.6, and (d) C1.0 samples at 28 d of curing (A: alite, B: belite, C: calcite, E: ettringite, F: ferrite, P: portlandite, Q: quartz).

ture and the dehydration of ettringite and C–S–H [39]. The second and third ranges are attributed to the dehydroxylation and decarbonation of $Ca(OH)_2$ and $CaCO_3$, respectively [39]. The effects of carbonation curing on the transformation of the hydrates are shown in Fig. 7. The high amounts of C–S–H, ettringite, and $Ca(OH)_2$ decreased from the non-carbonated to partially and fully carbonated samples because of the carbonation reaction [26]. Based on the TG/DTG test results, the weight losses of the samples in the above-mentioned three temperature regions are summarized in Table 2. In addition, the CO_2 uptake levels were calculated based on the decarbonation of $CaCO_3$ in the temperature range of 650 °C-750 °C. The results show that the CO_2 uptake level increased with the carbonation extent, reaching 8.97%, 8.76%, 6.90%, and 10.57% in CO_2 uptake levels in the fully-carbonated C0.1, C0.3, C0.6, and C1.0 samples, respectively.

The carbonation degrees of the samples measured using the phenolphthalein indicator are shown in Table 3. The area without color change is the carbonated area, which is divided by the total cross-sectional area of the sample. The calculated ratio was used to determine the carbonation degree (Table 3). The results show that the carbonation degree increased with the number of carbonation curing days. In addition, the carbonation degree increased with the CNT amount. For example, the fully carbonated C0.1, C0.3, C0.6, and C1.0 samples indicated carbonation percentages of 41.0%, 65.9%, 85.9%, and 99.4%, respectively. This can be deduced from the formation of pores caused by the CNTs and the shape of the CNTs (i.e., hollow tubes) [20]. In addition, the carbonation degrees obtained are attributable to the high amount of water for ensuring the target flow. Thus, the carbonation degree agreed well with those obtained using the CO_2 uptake percentage based on the TG/DTG curves, as summarized in Table 2.

The calculated CO_2 emission level and environmental impact are summarized in Table 4. The CO_2 uptake values obtained from the TG/DTG test results were used to evaluate the benefits of CO_2 reduction via the CO_2 curing method. Here, the CO_2 emission of PC was assumed to be 706 kg per ton of PC [14]. Furthermore, the CO_2 emissions calculated (as shown in Table 4) do not consider the effects of crushing, milling, transportation, and the production of other materials. Table 4 shows that the amount of CO_2 emissions is reduced as the carbonation curing progresses. Moreover, the incorporation of high amounts of CNTs, which increased the CO_2 uptake amount, reduced the net CO_2 emission from 506.7 to 490.7, 474.9, and 419.3 kg/ton in partially-carbonated and 473.1 to 462.7, 460.3, and 404.5 kg/ton in the fully-carbonated C0.1, C0.3, C0.6, and C1.0 samples, respectively. Thus, the environmental impact reduction are calculated to be 2.62%, 3.37%, 4.06%, and 7.51% in the partially-carbonated C0.1, C0.3, C0.6, and C1.0 samples, respectively. And, they increase to 9.08%, 8.87%, 7.00%, and 10.76% in the fully-carbonated samples, respectively. Hence, it can be said that the addition of CNT with carbonation curing not only achieves the functional properties, but also reduces the CO_2 emission amount.

3.3. Electrical heating performance of the samples

The C0.6 and C1.0 samples were subjected to the electrical heating tests because of their favorable electrical resistivity (i.e., <150 Ω cm), as shown in Fig. 2 [19]. As reported by Jang et al. good electrical conductivity is required if CNT/cement composites are to be used as electrical heating systems [19]. If the composites exhibit high electrical resistivity, then a high input voltage is required to heat them, which causes problems such as high energy consumption and thermal shock [19]. The temperature was increased during the cyclic heating tests, as shown in Fig. 8. Based on the previous study, conductive CNT networks can be redistributed
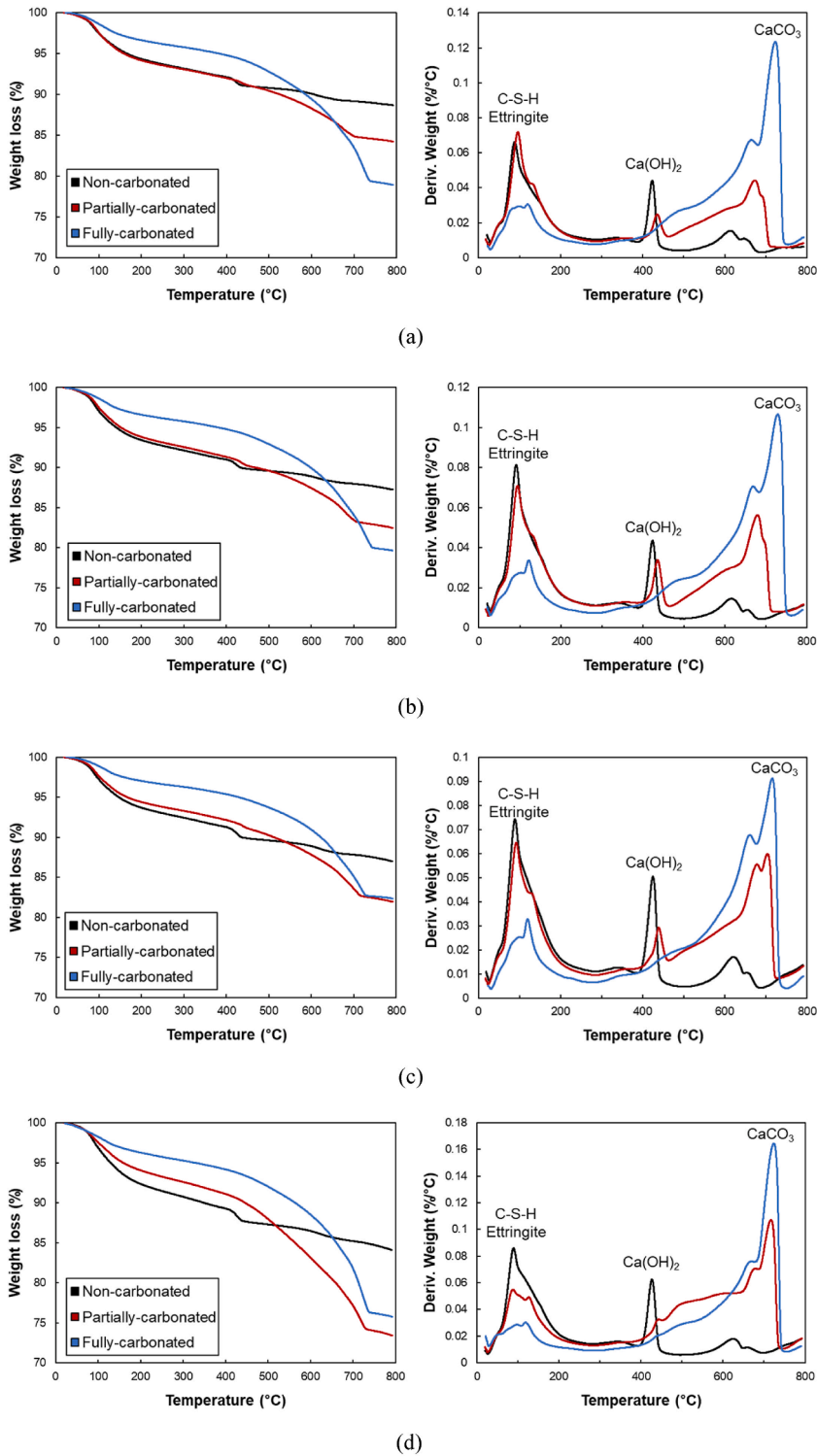
Fig. 7. TG and DTG test results of (a) C0.1, (b) C0.3, (c) C0.6, and (d) C1.0 samples.

during the heating process, which continues as the number of heating cycles increases [40]. This occurs because individual CNTs expand as the composite is heated, which reduces the electrical resistivity (i.e., the negative temperature coefficient (NTC) effect). Subsequently, the cement matrix expands, and the distance between adjacent CNT increases, thereby increasing the electrical resistivity (i.e., the positive temperature coefficient (PTC) effect) [40]. Hence, the electrical heating performance of the samples decreased regardless of the CNT amount. However, the temperature performance of the C1.0 samples decreased significantly compared with that
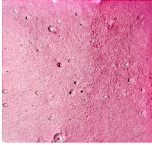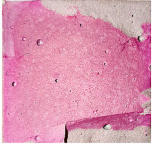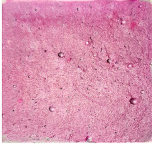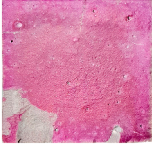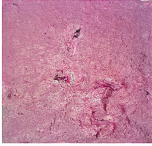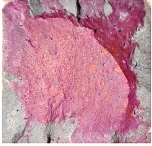
Table 2
Weight loss of the samples obtained from TG curves (%).

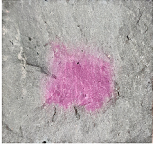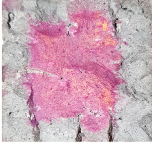| Sample		Below 200 °C (H$_2$O and AFt/AFm)	400-450 °C (Ca(OH)$_2$)	600-750 °C (CaCO$_3$)	CO$_2$ uptake
C0.1	N	5.68	1.11	1.17	–
	P	5.85	0.87	3.76	2.59
	F	3.43	0.8	10.14	8.97
C0.3	N	6.56	1.16	1.25	–
	P	6.16	1.11	4.58	3.33
	F	3.39	0.74	10.01	8.76
C0.6	N	6.31	1.39	1.43	–
	P	5.61	1.02	5.43	4.00
	F	2.98	0.71	8.33	6.90
C1.0	N	7.62	1.66	1.76	–
	P	5.93	1.23	9.14	7.38
	F	3.71	0.86	12.33	10.57

*N, P, F denote 'Non-carbonated', 'Partially-carbonated', and 'Fully-carbonated', samples respectively.

Table 3
Carbonation degree of the samples based on phenolphthalein indicator.

Sample code	Carbonation curing days		
	Non-carbonated	Partially-carbonated	Fully-carbonated
C0.1			
Carbonation degree	0%	18.5%	41.0%
C0.3			
Carbonation degree	1.3%	11.9%	65.9%
C0.6			
Carbonation degree	1.8%	29.7%	85.9%
C1.0			
Carbonation degree	1.5%	62.8%	99.4%

of the C0.6 samples. As shown in Fig. 8, the temperature of the C1.0 samples increases by approximately 60 °C. This indicates that the surface of the samples is approximately 70 °C, and considering the temperature gradient in the cementitious composites, the internal temperature is 90 °C-100 °C [19]. The internal temperature of the C1.0 samples during the first two heating cycles was higher than that of the C0.6 samples; therefore, more thermal expansion occurred in the C1.0 samples, which would affect the redistribution of the conductive CNT networks. Meanwhile, the relationship between the period of carbonation curing and the electrical heating performances of the C0.6 and C1.0 samples can be determined based on Fig. 8. During the first heating cycle, the temperatures of the non, partially, and fully-carbonated C0.6 samples increased by 35.1 °C 39.1 °C, and 38.6 °C, respectively. By the 10th heating cycle, these values were 28.4 °C, 22.6 °C, and 23.6 °C, corresponding to decrease percentages of 18.9%, 42.2%, and 38.8%, respectively. Similarly, during the first heating cycle, the temperatures of the non-, partially, and fully carbonated C1.0 samples increased by 53.4 °C, 54.3 °C, and 56.7 °C, respectively. By the 10th heating cycle, these values were 34.3 °C, 34.7 °C, and 27.0 °C, corresponding to decrease percentages of 35.8%, 36.0%, and 52.3%, respectively. To investigate these results systematically, variations in the electrical resistivity during the cyclic heating test were examined, as shown in Fig. 9. The electrical resistivity increased during the test

Table 4

Calculated CO_2 emission level and environmental impact.

Sample		CO_2 emission from cement (kg/ton)	CO_2 uptake in samples (kg/ton)	Final CO_2 emission (kg/ton)	Environmental impact reduction (%)
C0.1	N	526.4	6.2	502.3	0.0
	P	526.4	19.8	506.7	2.62
	F	526.4	53.4	473.1	9.08
C0.3	N	514.2	6.4	507.8	0.0
	P	514.2	23.6	490.7	3.37
	F	514.2	51.5	462.7	8.87
C0.6	N	502.1	7.2	494.9	0.0
	P	502.1	27.3	474.9	4.06
	F	502.1	41.8	460.3	7.00
C1.0	N	461.4	8.1	453.3	0.0
	P	461.4	42.2	419.3	7.51
	F	461.4	56.9	404.5	10.76

*N, P, F denote 'Non-carbonated', 'Partially-carbonated', and 'Fully-carbonated', samples respectively.
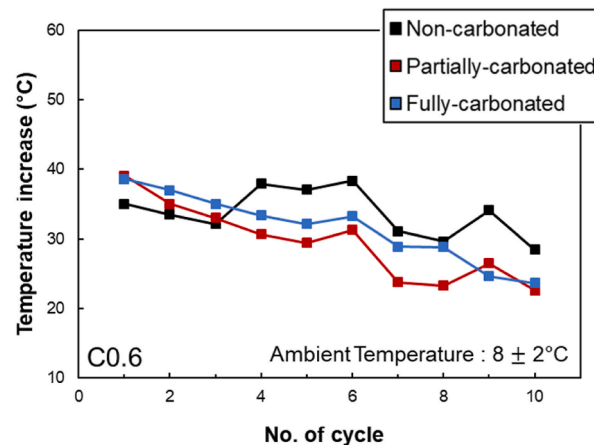
(a)
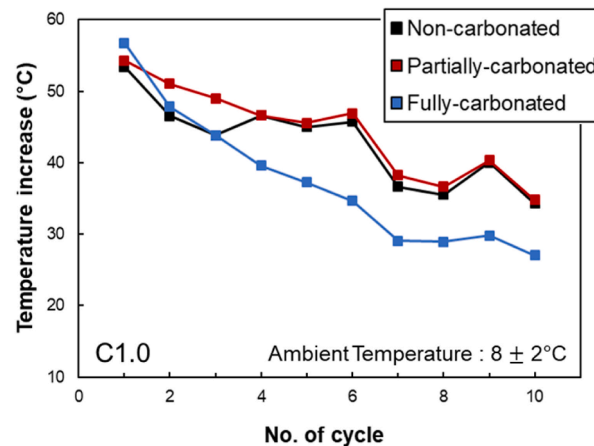
(b)

Fig. 8. Maximum temperature increase of (a) C0.6 and (b) C1.0 samples during cyclic heating test.

because of heat, which induced additional hydration in the cement matrix [40]. However, the change in the electrical resistivity of the samples depended on the number of carbonation curing days. In the non, partially, and fully-carbonated C0.6 samples, the electrical resistivity increased from 44.1, 48.9, and 46.9 Ω cm, to 57.3, 72.3, and 67.2 Ω cm, which correspond to increase percentages of 30.1%, 47.6%, and 43.2%, respectively. Similarly, in the non, partially, and fully carbonated C1.0 samples, the electrical resistivity increased from 25.3, 31.5, and 38.4 Ω cm, to 38.9, 43.9, and 91.8 Ω cm, which correspond to increase percentages of 57.7%, 39.7%, and 112.9%, respectively. In the samples cured via carbonation, the carbonation-induced hydrates can increase the distance between
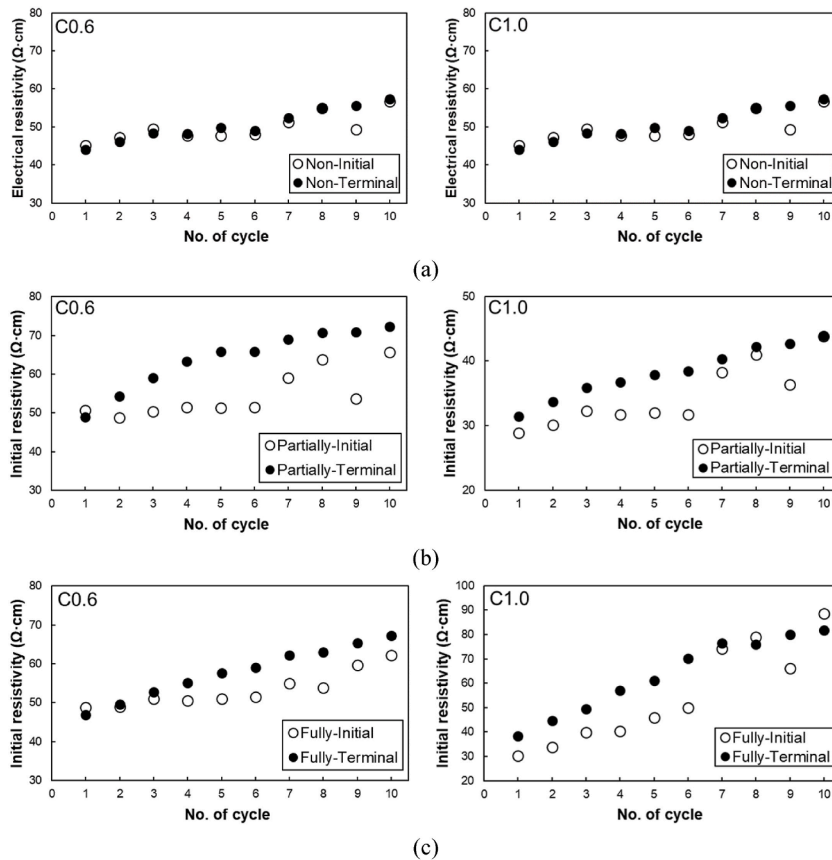
Fig. 9. Heat-induced electrical resistivity in (a) non, (b) partially, and (c) fully-carbonated C0.6 and C1.0 samples.

adjacent CNTs and/or hinder the formation of conductive CNT networks. Thus, the redistribution of CNTs by the heating mechanism can be regarded as more significant in the samples that underwent carbonation curing. Hence, the temperature of the samples that underwent carbonation curing increased less as compared with that of the samples without carbonation (Fig. 9). The detrimental effects of carbonation curing on the electrical heating capacity of CNT/cement composites can be ameliorated by introducing micro-sized conductive fillers. A previous study indicated that the inclusion of carbon fibers with micro-scale dimensions can help prevent the disruption of CNT-based conductive networks, thus ensuring stable connections within the composite [41,42]. As such, the incorporation of carbon fibers represents a potential solution for mitigating the degradation of electrical heating capabilities in CNT/cement composites subjected to carbonation curing.

The long-term heating performances of the C0.6 and C1.0 samples are shown in Fig. 10. The surface temperature results can be classified into two regions: before and after 3 h. For the first 1 h, the surface temperature of all the samples increased. After 1 h of heating, the surface temperature of some samples (e.g., non-carbonated C0.6, non-carbonated C1.0, and partially-carbonated C1.0) decreased up to 3 h. After 3 h, the surface temperature of each sample stabilized for an additional 17 h. This can be explained by the expansion of individual CNT and the cement matrix, as discussed above. The expansion of CNT and the cement matrix can disrupt the conductive CNT networks, thus causing changes in the temperature, as shown in Fig. 10. Furthermore, the extent to which the networks are disturbed contributes to the difference in the temperature variation between the sample types. The non-carbonated samples showed a greater decrease in temperature before it stabilized compared with the partially or fully-carbonated samples. The non-carbonated C0.6 and C1.0 samples were heated to 52.2 °C and 61.5 °C, and then cooled and stabilized at 42.8 °C and 50.1 °C, respectively. This represents fractional decreases in the surface temperature of approximately 18.0% and 18.5%, respectively. By contrast, the partially and fully carbonated C0.6 samples were heated to 46.8 °C and 46.2 °C, respectively, and then cooled and stabilized at 42.8 °C. This represents fractional decreases in the surface temperature of approximately 8.5% and 7.4%, respectively. Similarly, the partially and fully-carbonated C1.0 samples were heated to 56.7 °C and 59.7 °C, and then cooled to 50.0 °C and 54.9 °C, respectively. This represents fractional decreases in the surface temperature of approximately 11.8% and 8.2%, respectively. The effects of the extent of carbonation on the long-term electrical heating performance were investigated based on variations in the electrical stability and electrical resistivity of the samples during the long-term heating process, as shown in Fig. 11. First, the electrical resistivity of the samples decreased regardless of the CNT amount and/or number of carbonation curing days. This was caused by the NTC effect [43]. Subsequently, the electrical resistivity increased because of the PTC effect. All samples, regardless of type, showed both NTC and PTC effects; however, the extent at which the PTC effect occurred depended on the number of carbonation curing days. The electrical re-
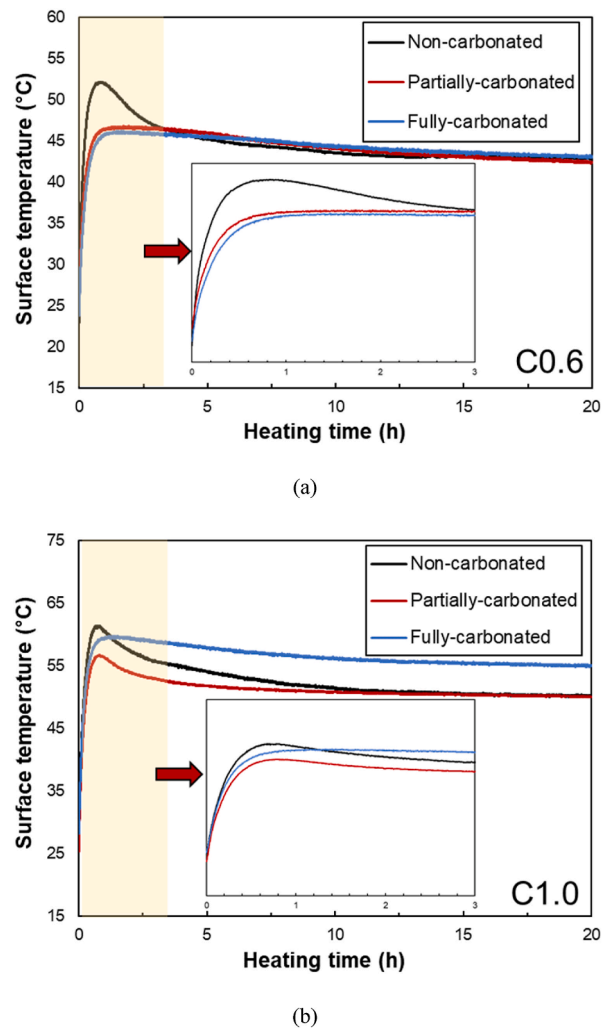
(a)

(b)

Fig. 10. Electrical heating stability of the samples during long-term heating tests.

sistivity decreased less as the number of carbonation curing days increased, indicating that the PCT effect was less prominent in the fully carbonated samples than in the partially carbonated and non-carbonated samples. It can be inferred that the samples became denser after carbonation curing owing to carbonation-induced hydrates. Consequently, the disturbance of the conductive CNT networks caused by the expansion of CNT was mitigated. Thus, carbonation curing can potentially improve the electrical heating stability of the CNT/cement composites during long-term heating.

Based on the experimental findings of the present study, it is possible to conclude that the use of carbonation curing in the fabrication of cementitious composites has the potential to create functional materials that effectively trap CO_2 while maintaining their intended functionality. However, excessive extent of carbonation curing has been shown to induce a negative impact on the electrical and thermal conductivities of these composites, leading to a decrease in their functional capabilities. As such, it is required to identify and implement appropriate carbonation curing regimes when creating cementitious composites for specific functional purposes such as cement-based sensors, electrical heating systems, or electromagnetic wave interference composites.

4. Concluding remarks

In this study, the effects of CO_2 curing regime on the characterization, physicochemical properties and electrical heating performance of CNT/cement composites were investigated. It was found that the carbonation curing regime affected the electrical and thermal conductivity, and compressive strength of the samples, and the effect of carbonation differed depending on the amount of CNT. Especially, the incorporation of CNT accelerated the carbonation curing reaction, increased the CO_2 uptake levels, and decreased the CO_2 emissions, thereby increasing the environmental impact up to 10.76% in the sample incorporating CNT 1.0% and cured under the fully-carbonated condition. From the electrical heating test, it was found that the carbonated products can disturb the connections of CNT-based conductive networks, thereby degrading their electrical heating performance. In this context, it can be concluded that
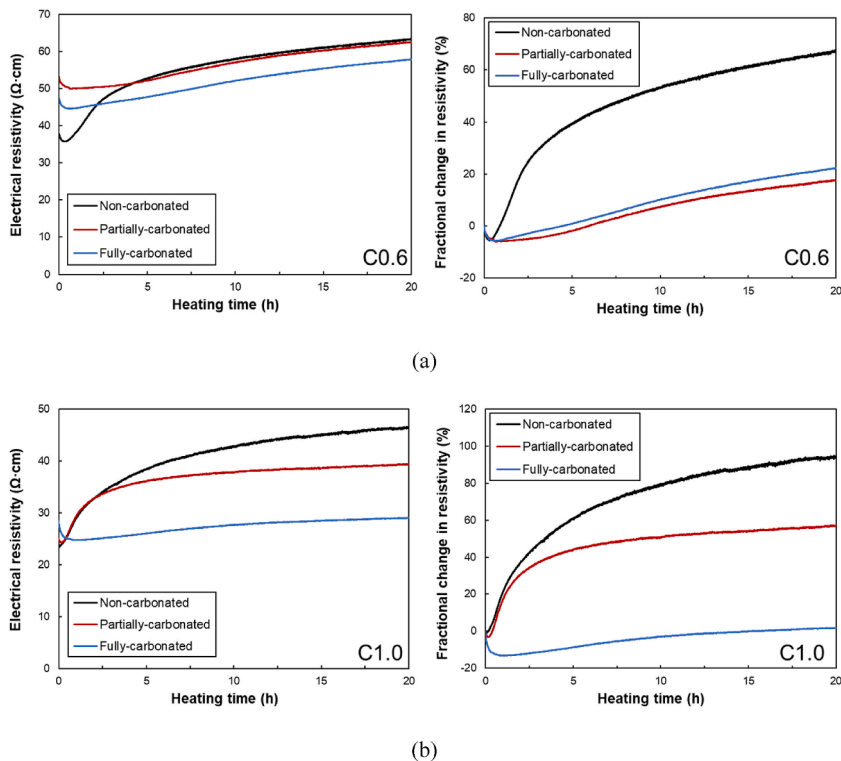
(a)

(b)

Fig. 11. Electrical resistivity and fractional change in resistivity of (a) C0.6 and (b) C1.0 samples.

the appropriate carbonation curing regime is required to ensure the desired functional properties, and an addition of conductive fillers larger than the CNT is expected to mitigate the degradation in their functional capabilities after carbonation curing.

CRediT authors' statement

Deaik Jang: Conceptualization, Methodology, Formal analysis, Investigation, Writing - Original Draft, Writing - Review & Editing.
H.N. Yoon: Methodology, Investigation, Experiment.
Joonho Seo: Formal analysis, Investigation, Review & Editing.
Beomjoo Yang: Methodology, Formal analysis, Investigation.
Jeong Gook Jang: Methodology, Experiment, Review & Editing, Funding acquisition.
Solmoi Park: Investigation, Writing - Review & Editing, Project administration, Funding acquisition.

Declaration of competing interest

The authors declare that they have no known competing financial interests or personal relationships that could have appeared to influence the work reported in this paper.

Data availability

Data will be made available on request.

Acknowledgments

References

[1] Q. Liu, R. Gao, V.W.Y. Tam, W. Li, J. Xiao, Strain monitoring for a bending concrete beam by using piezoresistive cement-based sensors, Construct. Build. Mater. 167 (2018) 338–347, https://doi.org/10.1016/j.conbuildmat.2018.02.048.
[2] J. Seo, D. Jang, B. Yang, H.N. Yoon, J.G. Jang, S. Park, H.K. Lee, Material characterization and piezoresistive sensing capability assessment of thin-walled CNT-embedded ultra-high performance concrete, Cem. Concr. Compos. 134 (2022) 104808, https://doi.org/10.1016/j.cemconcomp.2022.104808.
[3] Y.C. Choi, Cyclic heating and mechanical properties of CNT reinforced cement composite, Compos. Struct. 256 (2021) 113104, https://doi.org/10.1016/j.compstruct.2020.113104.

[4] H.N. Yoon, D. Jang, T. Kil, H.K. Lee, Influence of various deterioration factors on the electrical properties of conductive cement paste, Construct. Build. Mater. 367 (2023) 130289, https://doi.org/10.1016/j.conbuildmat.2022.130289.

[5] D. Jang, B.H. Choi, H.N. Yoon, B. Yang, H.K. Lee, Improved electromagnetic wave shielding capability of carbonyl iron powder-embedded lightweight CFRP composites, Compos. Struct. 286 (2022) 115326, https://doi.org/10.1016/j.compstruct.2022.115326.

[6] X. Wang, Q. Li, H. Lai, Y. Peng, S. Xu, Broadband microwave absorption enabled by a novel carbon nanotube gratings/cement composite metastructure, Compos. B Eng. 242 (2022) 110071, https://doi.org/10.1016/j.compositesb.2022.110071.

[7] A. Abolhasani, A. Pachenari, S. Mohammad Razavian, M. Mahdi Abolhasani, Towards new generation of electrode-free conductive cement composites utilizing nano carbon black, Construct. Build. Mater. 323 (2022) 126576, https://doi.org/10.1016/j.conbuildmat.2022.126576.

[8] W. Dong, W. Li, X. Zhu, D. Sheng, S.P. Shah, Multifunctional cementitious composites with integrated self-sensing and hydrophobic capacities toward smart structural health monitoring, Cem. Concr. Compos. 118 (2021) 103962, https://doi.org/10.1016/j.cemconcomp.2021.103962.

[9] P. Vizureanu, N. Cimpoesu, V. Radu, M. Agop, Investigations on thermal conductivity of carbon nanotubes reinforced composites, Exp. Heat Tran. 28 (2015) 37–57, https://doi.org/10.1080/08916152.2013.803176.

[10] D. Jang, J. Bang, H.N. Yoon, J. Seo, J. Jung, Deep learning - based LSTM model for prediction of long - term piezoresistive sensing performance of cement - based sensors incorporating multi - walled carbon nanotube, Comput. Concr. 30 (2022) 301–310, https://doi.org/10.12989/cac.2022.30.5.301.

[11] D. Jang, H.N. Yoon, B. Yang, H.R. Khalid, Cyclic heat-generation and storage capabilities of self-heating cementitious composite with an addition of phase change material, Construct. Build. Mater. 369 (2023) 130512, https://doi.org/10.1016/j.conbuildmat.2023.130512.

[12] H.K. Kim, I.S. Park, H.K. Lee, Improved piezoresistive sensitivity and stability of CNT/cement mortar composites with low water-binder ratio, Compos. Struct. 116 (2014) 713–719, https://doi.org/10.1016/j.compstruct.2014.06.007.

[13] B. Han, X. Yu, E. Kwon, J. Ou, Effects of CNT concentration level and water/cement ratio on the piezoresistivity of CNT/cement composites, J. Compos. Mater. 46 (2012) 19–25, https://doi.org/10.1177/0021998311401114.

[14] J. Bae, S. Kim, I.T. Amr, J. Seo, D. Jang, R. Bamagain, B.A. Fadhel, E. Abu-aisheh, H.K. Lee, Evaluation of physicochemical properties and environmental impact of environmentally amicable Portland cement/metakaolin bricks exposed to humid or CO2 curing condition Jin-Ho, J. Build. Eng. 47 (2022) 103831, https://doi.org/10.1016/j.jobe.2021.103831.

[15] T. Chen, X. Gao, Use of carbonation curing to improve mechanical strength and durability of pervious concrete, ACS Sustain. Chem. Eng. 8 (2020) 3872–3884, https://doi.org/10.1021/acssuschemeng.9b07348.

[16] T. Chen, X. Gao, Effect of carbonation curing regime on strength and microstructure of Portland cement paste, J. CO2 Util. 34 (2019) 74–86, https://doi.org/10.1016/j.jcou.2019.05.034.

[17] H.K. Lee, I.W. Nam, M. Tafesse, H.K. Kim, Fluctuation of electrical properties of carbon-based nanomaterials/cement composites: case studies and parametric modeling, Cem. Concr. Compos. 102 (2019) 55–70, https://doi.org/10.1016/j.cemconcomp.2019.04.008.

[18] K. Gawel, S. Wenner, L. Edvardsen, Effect of carbonation on bulk resistivity of cement/carbon nanofiber composites, Construct. Build. Mater. 305 (2021) 124794, https://doi.org/10.1016/j.conbuildmat.2021.124794.

[19] D. Jang, H.N. Yoon, J. Seo, H.K. Lee, G.M. Kim, Effects of silica aerogel inclusion on the stability of heat generation and heat-dependent electrical characteristics of cementitious composites with CNT, Cem. Concr. Compos. 115 (2021) 103861, https://doi.org/10.1016/j.cemconcomp.2020.103861.

[20] D. Jang, H.N. Yoon, S.Z. Farooq, H.K. Lee, I.W. Nam, Influence of water ingress on the electrical properties and electromechanical sensing capabilities of CNT/ cement composites, J. Build. Eng. 42 (2021) 103065, https://doi.org/10.1016/j.jobe.2021.103065.

[21] H.K. Kim, I.W. Nam, H.K. Lee, Enhanced effect of carbon nanotube on mechanical and electrical properties of cement composites by incorporation of silica fume, Compos. Struct. 107 (2014) 60–69, https://doi.org/10.1016/j.compstruct.2013.07.042.

[22] G.M. Kim, I.W. Nam, H.N. Yoon, H.K. Lee, Effect of superplasticizer type and siliceous materials on the dispersion of carbon nanotube in cementitious composites, Compos. Struct. 185 (2018) 264–272, https://doi.org/10.1016/j.compstruct.2017.11.011.

[23] M.J. Lim, H.K. Lee, I.W. Nam, H.K. Kim, Carbon nanotube/cement composites for crack monitoring of concrete structures, Compos. Struct. 180 (2017) 741–750, https://doi.org/10.1016/j.compstruct.2017.08.042.

[24] M. Tafesse, N. Kon, A. Shiferaw, H. Kyoung, S. Wook, H. Kim, Flowability and electrical properties of cement composites with mechanical dispersion of carbon nanotube, Construct. Build. Mater. 293 (2021) 123436, https://doi.org/10.1016/j.conbuildmat.2021.123436.

[25] J.G. Jang, H.K. Lee, Microstructural densification and CO2 uptake promoted by the carbonation curing of belite-rich Portland cement, Cement Concr. Res. 82 (2016) 50–57, https://doi.org/10.1016/j.cemconres.2016.01.001.

[26] S.M. Park, J.G. Jang, Carbonation-induced weathering effect on cesium retention of cement paste, J. Nucl. Mater. 505 (2018) 159–164, https://doi.org/10.1016/j.jnucmat.2018.04.015.

[27] D.I. Jang, H.N. Yoon, I.W. Nam, H.K. Lee, Effect of carbonyl iron powder incorporation on the piezoresistive sensing characteristics of CNT-based polymeric sensor, Compos. Struct. 244 (2020) 112260, https://doi.org/10.1016/j.compstruct.2020.112260.

[28] B.H. Manan Bhandari, Jianchao Wang, Daeik Jang, IlWoo Nam, A comparative study on the electrical and piezoresistive sensing characteristics of GFRP and CFRP composites with hybridized incorporation of carbon nanotubes, graphenes, carbon nanofibers, and graphite nanoplatelets, Sensors 21 (2021) 7291, https://doi.org/10.3390/s21217291.

[29] D. Jang, T. Kil, H.N. Yoon, J. Seo, H.R. Khalid, Artificial neural network approach for predicting tunneling-induced and frequency-dependent electrical impedances of conductive polymeric composites, Mater. Lett. 302 (2021) 130420, https://doi.org/10.1016/j.matlet.2021.130420.

[30] J. Seo, S.J. Bae, D.I. Jang, S. Park, B. Yang, H.K. Lee, Thermal behavior of alkali-activated fly ash/slag with the addition of an aerogel as an aggregate replacement, Cem. Concr. Compos. 106 (2020) 103462, https://doi.org/10.1016/j.cemconcomp.2019.103462.

[31] R. Snellings, J. Chwast, Ö. Cizer, N. De Belie, Y. Dhandapani, P. Durdzinski, J. Elsen, J. Haufe, D. Hooton, C. Patapy, M. Santhanam, K. Scrivener, D. Snoeck, L. Steger, S. Tongbo, A. Vollpracht, F. Winnefeld, B. Lothenbach, RILEM TC-238 SCM recommendation on hydration stoppage by solvent exchange for the study of hydrate assemblages, Mater. Struct. Constr. 51 (2018), https://doi.org/10.1617/s11527-018-1298-5.

[32] F. Naeem, H.K. Lee, H.K. Kim, I.W. Nam, Flexural stress and crack sensing capabilities of MWNT/cement composites, Compos. Struct. 175 (2017) 86–100, https://doi.org/10.1016/j.compstruct.2017.04.078.

[33] I.W. Nam, H. Souri, H.K. Lee, Percolation threshold and piezoresistive response of multi-wall carbon nanotube/cement composites, Smart Struct. Syst. 18 (2016) 217–231, https://doi.org/10.12989/sss.2016.18.2.217.

[34] I.W. Nam, H.K. Lee, Image analysis and DC conductivity measurement for the evaluation of carbon nanotube distribution in cement matrix, Int. J. Concr. Struct. Mater. 9 (2015) 427–438, https://doi.org/10.1007/s40069-015-0121-8.

[35] W.S. Bao, S.A. Meguid, Z.H. Zhu, G.J. Weng, Tunneling resistance and its effect on the electrical conductivity of carbon nanotube nanocomposites, J. Appl. Phys. 111 (2012), https://doi.org/10.1063/1.4716010.

[36] M. Jung, J. Park, S. gul Hong, J. Moon, Electrically cured ultra-high performance concrete (UHPC) embedded with carbon nanotubes for field casting and crack sensing, Mater. Des. 196 (2020) 109127, https://doi.org/10.1016/j.matdes.2020.109127.

[37] B. Han, L. Zhang, S. Sun, X. Yu, X. Dong, T. Wu, J. Ou, Electrostatic self-assembled carbon nanotube/nano carbon black composite fillers reinforced cement-based materials with multifunctionality, Composer Part A Appl. Sci. Manuf. 79 (2015) 103–115, https://doi.org/10.1016/j.compositesa.2015.09.016.

[38] J.G. Jang, S.M. Park, G.M. Kim, H.K. Lee, Stability of MgO-modified geopolymeric gel structure exposed to a CO2-rich environment, Construct. Build. Mater. 151 (2017) 178–185, https://doi.org/10.1016/j.conbuildmat.2017.06.088.

[39] D. Jang, H.N. Yoon, J. Seo, B. Yang, Effects of exposure temperature on the piezoresistive sensing performances of MWCNT-embedded cementitious sensor, J. Build. Eng. 47 (2022) 103816, https://doi.org/10.1016/j.jobe.2021.103816.

[40] G.M. Kim, F. Naeem, H.K. Kim, H.K. Lee, Heating and heat-dependent mechanical characteristics of CNT-embedded cementitious composites, Compos. Struct. 136 (2016) 162–170, https://doi.org/10.1016/j.compstruct.2015.10.010.

[41] G.M. Kim, H.N. Yoon, H.K. Lee, Autogenous shrinkage and electrical characteristics of cement pastes and mortars with carbon nanotube and carbon fiber, Construct. Build. Mater. 177 (2018) 428–435, https://doi.org/10.1016/j.conbuildmat.2018.05.127.

[42] G.M. Kim, B.J. Yang, H.N. Yoon, H.K. Lee, Synergistic effects of carbon nanotube and carbon fiber on heat generation and electrical characteristics of

cementitious composites, Carbon N. Y. 134 (2018) 283–292, https://doi.org/10.1016/j.carbon.2018.03.070.

[43] D. Jang, H.N. Yoon, S. Park, S. Kim, J.H. Bae, N. Kim, G.M. Kim, J. Seo, Pressure-aided fabrication of CNT-incorporated composites made with fly ash or slag-blended Portland cement, Compos. Struct. 313 (2023) 116926, https://doi.org/10.1016/j.compstruct.2023.116926.